

# Synthesis and Characterization of Poly-Methacrylic Acid Grafted Chitosan-Bentonite Composite and its Application for Heavy Metals Recovery

M.A. Abdel Khalek<sup>1\*</sup>, Ghada A. Mahmoud<sup>2</sup> and Nabil A. El-Kelesh<sup>2</sup>

1. Central Metallurgical R & D Institute, (CMRDI) P.O. Box 87, Helwan, Cairo, Egypt.

2. National Center for Radiation Research and Technology, P.O. Box 29, Nasr City, Cairo, Egypt

\* E-mail of the corresponding author: [kalekma@yahoo.com](mailto:kalekma@yahoo.com)

## Abstract

Poly-methacrylic acid grafted chitosan-bentonite nanocomposite (MACB) was synthesized by  $\gamma$ -irradiation polymerization. The nanocomposite was characterized by Fourier transform infrared (FTIR) spectroscopy, X-ray diffraction (XRD) crystallography, thermal gravimetric analysis (TGA) and scanning electron microscopy (SEM). The MACB nanocomposite was employed for the adsorption of mercury, cadmium and lead ions from aqueous solution. The effect of various parameters such as pH, contact time, metal ion concentration and temperature on the adsorption of metal ions onto MACB nanocomposite was investigated. The experimental results indicated that the order of adsorption capacity of MACB nanocomposite for metal ions was as follows:  $Hg^{2+} > Pb^{2+} > Cd^{2+}$ . The data indicating that the adsorption of the latter ions onto MACB nanocomposite followed both the Langmuir and Freundlich isotherm models. Equilibrium adsorption isotherm fitted the Langmuir model for  $Hg^{2+}$  ions and the adsorption of  $Cd^{2+}$  ions better fit the Freundlich isotherm model. The adsorption of  $Pb^{2+}$  ions followed both the Langmuir and Freundlich isotherm models.

**Keywords:** hydrogel; nanocomposites; clay; chitosan;  $\gamma$ -ray irradiation; Metal uptake

## 1. Introduction

Natural polymers have been studied as possible materials for superabsorbent hydrogels due to their biodegradability and wide availability. Chitosan is a high molecular weight polysaccharide composed mainly of  $\beta$ -(1,4)-linked 2-deoxy-2-aminod-glucopyranose units and partially of  $\beta$ -(1,4)-linked 2-deoxy- 2-acetamido-d-glucopyranose. Chitosan is inexpensive as well as nontoxic and exhibits high mechanical strength, hydrophilic character, good adhesion, etc. Thus chitosan are used as a food additive, a supporting material for chromatography and a chelating polymer for heavy metals removal (Guibal et al., 1999, Tianwei et al., 2001 and Han et al., 2010). Interest in the modification of chitosan through graft copolymerization has grown significantly. The combination of natural and synthetic polymers via grafting yields hybrid materials which may produce desirable properties.

Clay is a natural raw material that has been used for various purposes for ages and its dimension is under 2 mm. Montmorillonite is a member of smectite group clay minerals. Bentonites have a high content of montmorillonite and contain fewer amounts of other clay minerals. Bentonite clay (hydrated aluminum silicate) was shown to be efficient in the removal of many toxic metal ions such as lead, cobalt, nickel, copper, zinc, cadmium and uranium in aqueous solutions (Bailliez et al., 2004, Smiciklas et al., 2006, Mobasherpour et al., 2011, Corami et al., 2007, Zhu et al., 2008 and Simon et al., 2008). However, after adsorption of metal ions, it is not easy to separate the suspended fine solids of bentonite from aqueous solution (Choi, 2008). Therefore, it is needed to bind bentonite with polymer to solve this problem. The polymer/clay nanocomposites have attracted extensive interests around the world because they combine the structure, physical, and chemical properties of both inorganic and organic materials. Compared to the pure polymers, these nanocomposite demonstrate excellent properties; such as improved storage modulus, decreased thermal expansion coefficients, reduced gas permeability, and enhanced ionic conductivity because of the larger filler/matrix interfacial surface area (Song et al., 2005, Seo et al., 2005, Yao et al., 2002, Sun, 2002, Vaia, 2000 and Ray et al., 2003). Water pollution by heavy metals through the discharge of industrial effluents, is a worldwide environmental problem. Studies have proved that the metals such as copper, lead, zinc, cobalt, nickel, chromium and mercury are considered to be toxic. Cobalt containing compound are widely used in many industrial

applications such as mining, metallurgical, paints, pigments and electronics (Ghassabzadeh et al., 2010). Small amount of cobalt is essential for human health because it is a part of vitamin B<sub>12</sub>. However, higher concentration of cobalt may cause paralysis, diarrhoea, low blood pressure, lung irritation and bone defects. Nickel is being widely used in electroplating industries. It is also used in fertilizers. Exposure to nickel can cause dermatitis and allergic sensitization. Inhalation of Ni can cause respiratory cancer. Lead compound is widely used in painting, plastics and batteries. At low concentration lead can adversely affect the brain, the central nervous system, blood cells, and kidneys (Inglezakis et al., 2007). Therefore, removal methods of heavy metals from wastewater have been investigated considerably for past several years. A number of physical and chemical processes exists which include precipitation, solvent extraction, membrane processes, filtration, ion-exchange and adsorption. Among them, adsorption is an efficient and economical process. The efficiency of technique depends on the nature of adsorbent. The adsorbent such as activated carbon (Zaini et al., 2010), clay (Abu-Eishah, 2008), activated alumina (Bishnoi et al., 2004), chitosan (Paulino et al., 2007), silica (Aguado et al., 2009), zeolite (Motsi et al., 2009) and hydroxyapatite (Xu et al., 2008) were used for heavy metal removal.

In this study, we studied the modification of chitosan by  $\gamma$ -ray irradiation-induced graft copolymerization with methacrylic acid in acetic acid aqueous solution containing organophilic bentonite clay. MACB nanocomposite explored as an adsorbent for the removal of heavy metals such as lead, cobalt and nickel from aqueous solution. The reason behind choosing chitosan as a binding material for bentonite is its high abundance in nature and special characteristics such as hydrophilicity, biocompatibility, biodegradability, non-toxicity, adsorption properties, etc. The presence of amino and hydroxyl groups in chitosan can serve as the active sites for adsorption.

## 2. Materials and Methods

### 2.1. Materials

Methacrylic acid (MAA) and bentonite were obtained from Merck, Germany and used without further purification. Chitosan used throughout this study; was commercial and used as received. All other chemicals used were reagent grade and purchased from El-Nasr Co. for Chemical Industries (Egypt) and used as purchased without further purification.

### 2.2. Preparation of MACB Nanocomposites

The first part of the experiment a clear chitosan aqueous solution was prepared by dissolving the chitosan 1.0 % w/v in a 1% (v/v) acetic acid solution using a magnetic stirrer for 1 h at 60°C, followed by continuously stirring overnight at room temperature. After that, 20 wt% of MAA was added to it. The content was then stirred well using magnetic stirrer for 15 min. In the second part, the MACB nanocomposite was synthesized prior to the addition of bentonite. The pH of the solution was adjusted to 4.9 with NaOH in order to avoid any structural alteration of the phyllosilicate. On the other hand, an acidic pH value is necessary to provide NH<sub>3</sub><sup>+</sup> groups in the chitosan structure (Pandey et al., 2011). The bentonite was added to the solution in different percents range of 2–16% and was stirred well using magnetic stirrer for 30 min. The viscous mixture was transferred to a Petri dish and then they were irradiated at different irradiation doses range of 2-12 kGy, at room temperature, with a <sup>60</sup>Co source at a dose rate of 3.015 kGy/ h. The conversion percentage was determined gravimetrically by soaking the prepared hydrogels in water at 25°C for 24 h, as follows:-

$$\text{Conversion (\%)} = \frac{W_x}{W_0} \times 100 \quad (1)$$

Where W<sub>x</sub> is the weight of the dry gel after soaking in water and W<sub>o</sub> is the weight of the dry original gel.

### 2.3. Characterization

FTIR study was carried out on a FTIR 2000 spectrophotometer to analyze functional groups, using potassium

bromide (KBr) disk method and the morphology of adsorbents was investigated by FEI Quanta 200 scanning electron microscope operated at 20 kV accelerated voltage. XRD was performed on a X'Pert-Pro, PANalytical diffractometer operated at 30 kV/30 mA, to determine crystallinity of the material using Cu-K  $\alpha$  radiation with a wavelength of 1.54 Å in the wide angle region from 108 to 508 on  $2\theta$  scale.

#### 2.4. Adsorption Experiments

Stock solution (1000 mg/L) of each metal ion was prepared by dissolving required amount of nitrate salt of metal ion mercury, lead and cadmium obtained from Merck into double distilled water. The experimental solution of desired concentration was prepared by successive dilution of stock solution. In order to determine the effect of physicochemical parameters such as pH, adsorbent dose, contact time, initial metal ion concentration of solution and temperature. The adsorption experiments were performed by batch equilibrium method. The experiments were carried out in 150 ml of conical flasks by mixing a pre-weighed amount of adsorbent with 50 ml of metal ion solution. Initial pH of solutions was adjusted by 0.1 M NaOH or 0.1 M HNO<sub>3</sub>. All experiments were performed at room temperature and kept for stirring for a given period of time. Thereafter, the mixture was centrifuged (Remi Research centrifuge) and the initial and final metal ion concentrations were determined by Atomic Absorption Spectrophotometer (ECIL-4141). The removal percent of metal ion and amount of metal ion adsorbed on MACB nanocomposite ( $q_e$ ) was calculated by Eqs. (1) and (2), respectively:

$$\text{Removal}(\%) = \frac{(C_0 - C_e)}{C_0} \times 100 \quad (2)$$

Where  $C_0$  and  $C_e$  are the concentrations of the initial and equilibrium metal ions solution (mg/L), respectively.

$$q_e = \frac{(C_0 - C_e)V}{M} \quad (3)$$

Where  $q_e$  is the adsorption capacity of the nanocomposite (mg/g),  $V$  is the volume of the aqueous solution (L) and  $W$  is the mass of nanocomposite (g).

### 3. Results and Discussion

#### 3.1. Preparation

Figure 1 shows the dependence of the conversion percent of the prepared nanocomposite on the irradiation dose. The Figure shows that the conversion percent dramatically increases with the increase in irradiation dose up to 6 kGy due to the increase in the copolymerization between CT and MAA. After the conversion reached about, 92% at irradiation dose 6 kGy, the viscosity increases which restricted movement and thus the copolymerization is off.

#### 3.2. Characterization

The IR spectra of chitosan, bentonite and MACB nanocomposite were recorded in the region of 4000–500  $\text{cm}^{-1}$  and are shown in Fig.2. The spectrum of chitosan [Fig.2(a)] shows wide band around 3450  $\text{cm}^{-1}$  corresponding to amine N–H symmetrical vibration and H bonded O–H group. The peaks present on the range 3400–3800  $\text{cm}^{-1}$  were also corresponding to combination of characteristic peaks of O–H, NH<sub>2</sub> and intramolecular hydrogen bonding. The peaks at 2920 and 2320  $\text{cm}^{-1}$  are assigned to the symmetric and asymmetric –CH<sub>2</sub> vibrations of carbohydrate ring. The absorption peak at 1650  $\text{cm}^{-1}$  (C=O in amide group, amide I vibration), 1545  $\text{cm}^{-1}$  (–NH<sub>2</sub> bending of amide II) and 1390  $\text{cm}^{-1}$  (N–H stretching or C–N bond stretching vibrations, amide III vibration). The peak at 1092  $\text{cm}^{-1}$  corresponds to the symmetric stretching of C–O–C groups. The absorption peaks in the range 900–1200  $\text{cm}^{-1}$  are due to the antisymmetric C–O stretching from the pyranose ring and wagging of saccharide structure of chitosan (Pawlak et al., 2003).

The spectrum of bentonite [Fig.2(c)] shows the characteristic bands at 3640 and 3449  $\text{cm}^{-1}$  responsible for stretching vibrations of O–H, the band at 1112 and 1035  $\text{cm}^{-1}$  due to Si–O stretching (Rayanaud et al., 2002). The spectrum of MACB composite [Fig.2(b)] showed new absorption bands at 1700 and 1456  $\text{cm}^{-1}$  which were assigned to the stretching vibration of C=O and C–O of COOH groups of MAA, respectively. The peak of bentonite shifted from 1112 to 1092  $\text{cm}^{-1}$  due to interaction with chitosan. The stretching and bending vibration mode of –NH group of chitosan occurred at 3450 and 1650  $\text{cm}^{-1}$ , respectively which was overlapped with the bands of O–H groups in bentonite–chitosan composite.

XRD spectra of bentonite and MACB composite are presented in Fig.3. The crystalline peaks of bentonite at  $2\theta = 26.8, 31.98, 33.18, 34.28$  and  $39.98$  are also found in bentonite–chitosan composite with very small shifting in  $2\theta$ . This may be due to binding of bentonite with chitosan. This indicated that there was no marked change in the peak structure after the composite formation and confirmed that the crystal structure of bentonite is retained in MACB composite (Sundaram et al., 2008).

Figure 4 shows the morphology of bentonite and MACB composite. The bentonite powder exhibited as particles but in case of MACB composite aggregates appeared and film of chitosan over bentonite confirmed the formation of MACB composite. Surface of composite showed that the particles of bentonite were agglutinated on the surface and intercalating with network structure of copolymer. Therefore, the nanocomposite appeared the surface as a rough surface.

TGA curves of MAA grafted chitosan (MAC), bentonite and the MACB nanocomposites with different bentonite content are shown in Fig. 5. As shown from the Figure, the thermal stability of bentonite is high, only 13% of bentonite is decomposed until 600°C. Comparably, MAC shows low thermal stability and the remainder weight at 600°C is only 5%. TGA data exhibited a higher thermal decomposition temperature of MACB nanocomposite compared to MAC before it intercalate with bentonite which is undergo decomposition at relatively low temperature. Because inorganic species have good thermal stabilities, it is generally believed that the introduction of inorganic components into organic materials can improve their thermal stability. This increase in the thermal stability can be attributed to the high thermal stability of clay and to the interaction between the clay particles and the chitosan (Günister et al., 2007).

### 3.3. Metal Ions Adsorption Studies

#### 3.3.1. Effect of pH of Medium

The initial pH value of the solution is an important factor that must be considered during adsorption studies. Therefore, experiments were carried out to investigate the effect of pH on  $\text{Hg}^{2+}$ ,  $\text{Pb}^{2+}$  and  $\text{Cd}^{2+}$  removal by varying the pH from 2.0 to 7.0 and shown in Fig.6. It can be noted from Figure 6 the removal percent of metal ions was increased with the increase in initial pH of metal ions solution and the maximum value was reached at pH 6 for all metal ions investigated. However, it will decrement the removal percent of metal ions which may result from precipitation of metal ions in the form of their hydroxides (Afkhamia et al., 2010). At lower pH, the removal percent of metal ions decreased due to increased in the competition with  $\text{H}^+$  ions for active adsorption sites. These phenomena may be correlated with the dissociation constant pKa

of poly (acrylic acid) which is about 4.7 (Zheng, 2009). However, at higher pH value, presence of  $\text{H}^+$  ion in solution decreased and adsorbent surface also deprotonated, resulting in increasing the metal ions adsorption.

#### 3.3.2. Effect of Contact Time

Contact time is an important parameter because this factor can reflect the adsorption kinetics of an adsorbent for a given initial adsorbate concentration. Influence of contact time on adsorption of  $\text{Hg}^{2+}$ ,  $\text{Pb}^{2+}$  and  $\text{Cd}^{2+}$  onto MACB nanocomposite was investigated for the initial metal ion concentration of 100 mg/L for each metal ion and shown in Fig.7. The removal percent increased sharply within 30 min of contact time for all metal ions investigated thereafter no change was observed for  $\text{Hg}^{2+}$  ions. This established that the system has reached the equilibrium point but the rate slowed down for  $\text{Pb}^{2+}$  and  $\text{Cd}^{2+}$  ions until it reached the equilibrium point after 40 min. This depends on the difference in their ionic strength effects. As-prepared adsorbent belongs to hydrogels whose main feature is the

ability to absorb water quickly due to the hydrophilic networks. Hydrated polymer networks is formed at solid–liquid interface, thereby the diffusion from the aqueous solution into the MACB nanocomposite is started and bound immediately to the swollen polymeric networks as a result of electrostatic attraction. During this process, the swollen polymeric networks can diminish the diffusion, thus leading the adsorption system to reach equilibrium within a short time. Based on the above results, a contact time of 1 h was selected for all subsequent batch experiments. The removal efficiency of  $\text{Hg}^{2+}$ ,  $\text{Pb}^{2+}$  and  $\text{Cd}^{2+}$  was 94, 89 and 78 %, respectively.

### 3.3.3. Effect of Bentonite Content on Metal Ion Adsorption

Polymer–clay composites have received considerable interest. Clay minerals are low cost materials and the introduction of inorganic clay component can reduce the cost of material. Meanwhile, the interactions between them have effects on the properties of both clay and polymer systems. Figure 8 shows the effects of bentonite content on the removal of  $\text{Hg}^{2+}$ ,  $\text{Pb}^{2+}$  and  $\text{Cd}^{2+}$  ions. It is clear that the removal of metal ions increases with the increase in bentonite content up to 10 % after that decreasing occur. Generally, an appropriate addition of clay particles may improve the polymeric networks due to the higher swelling ratio of a hydrogel in aqueous solution which improve the adsorption. Also, the addition of bentonite can reduce the production cost of the adsorbents. This result indicates that the MACB nanocomposite containing 10% bentonite is the optimized system.

### 3.3.4. Effect of Equilibrium Metal Ion Concentration

The effect of different concentrations of  $\text{Hg}^{2+}$ ,  $\text{Pb}^{2+}$  and  $\text{Cd}^{2+}$  on the adsorption has been investigated. The adsorption capacities of MACB nanocomposite were given as a function of equilibrium concentration and shown in Fig. 9. It was clear the adsorption capacities of MACB nanocomposite increased with the increase in equilibrium metal ion concentration. Increasing equilibrium metal ion concentration may improve the driving force which overcomes the mass transfer resistance between solid- liquid phase (Anirudhan et al., 2010)[33]. The experimental results indicated that the order of adsorption capacity of MACB nanocomposite for metal ions was as follows:  $\text{Hg}^{2+} > \text{Pb}^{2+} > \text{Cd}^{2+}$ . These results were due to that the fluctuation motion of  $\text{Hg}^{2+} > \text{Pb}^{2+}$  and that which is greater than  $\text{Cd}^{2+}$  (Katima et al., 2001).

### 3.3.5. Adsorption Isotherm

An adsorption isotherm reveals the mathematical relationship between the adsorption capacity and equilibrium concentration of an adsorbent at a constant temperature. The most common types of isotherms are Langmuir and Freundlich models. The Langmuir isotherm assumes monolayer coverage of adsorbate onto a homogeneous adsorbent surface and can be expressed as:

$$\frac{C_e}{q_e} = \frac{C_e}{q_{\max}} + \frac{1}{b \cdot q_{\max}} \quad (4)$$

Where  $C_e$  is concentration of metal ions in solution at equilibrium (mg/L),  $q_e$  is the amount of metal ions at equilibrium in unit mass of adsorbent (mg/g),  $q_{\max}$  and  $b$  are the Langmuir coefficient related to adsorption capacity (mg/g) and adsorption energy (L/mg) respectively. These were determined from the slope and intercept of the plot of  $C_e/q_e$  against  $C_e$  as shown in Fig. 10. The Freundlich isotherm is based on adsorption on a heterogeneous surface and express by the following equation:

$$\ln q_e = \ln K_F + \left(\frac{1}{n}\right) \ln C_e \quad (5)$$

$K_F$  and  $n$  are the Freundlich coefficient related to adsorption capacity [ $\text{mg/g} (\text{mg/L})^{-1/n}$ ] and adsorption intensity of adsorbent, respectively. The values of  $n$  and  $K_F$  were calculated from the slope  $1/n$  and intercept  $\ln K_F$  of the plot of

In  $q_e$  against  $\ln C_e$  as shown in Fig.11. All the isotherm parameters were determined and correction coefficients are listed in Table 1. According to the correction coefficients of both Langmuir and Freundlich isotherm models (Table 1), it can be noted that the adsorption of  $Hg^{2+}$  ions fit the Langmuir isotherm model better than the Freundlich isotherm model but the adsorption of  $Cd^{2+}$  ions better fit the Freundlich isotherm model. On the other hand, the adsorption of  $Pb^{2+}$  ions followed both the Langmuir and Freundlich isotherm models. The values of  $n$  are greater than one which indicated favourable adsorption conditions (Hameed et al., 2008). In general, as the  $K_F$  value increases, the adsorption capacity of the adsorbent increases.

#### 4. Conclusions

Poly-methacrylic Acid grafted chitosan-bentonite nanocomposite (MACB) were successfully prepared by  $\gamma$ -irradiation techniques. The nanocomposite structure was confirmed by Fourier transform infrared (FTIR) spectroscopy, X-ray diffraction (XRD) crystallography, thermal gravimetric analysis (TGA) and scanning electron microscopy (SEM). TGA reveals that (MACB) nanocomposite exhibited better thermal stability compared to MAC due to the high rearrangement of the crystallinity form of (MACB) than MAC. The feasibility of using (MACB) nanocomposite for the removal of  $Hg^{2+}$ ,  $Pb^{2+}$  and  $Cd^{2+}$  metal ions from an aqueous solution was investigated. The maximum adsorption of heavy metal ions was obtained at pH 6 and at contact time of 30 minutes for mercury and 40 minutes for lead and cadmium. The experimental results indicated that the order of adsorption capacity of MACB composite for metal ions was as follows:  $Hg^{2+} > Pb^{2+} > Cd^{2+}$ . The data indicating that the adsorption of the latter ions onto MACB composite followed both the Langmuir and Freundlich isotherm models. Thus, the adsorption of  $Hg^{2+}$ ,  $Pb^{2+}$  and  $Cd^{2+}$  from onto Chitosan-Bentonite Composite are chemical and physical adsorption types.

#### References

- Abu-Eishah, S.I. (2008), "Voltammetric determination of analgesics using a montmorillonite modified electrode", *Appl. Clay Sci.* 42, 201-205.
- Afkhamia, A., Tehranib, M.S. & Bagherib, H. (2010), "Simultaneous removal of heavy-metal ions in wastewater samples using nano-alumina modified with 2,4-dinitrophenylhydrazine" *J. Hazard Materials*, 181, 836-844.
- Aguado, J., Arsuaga, J.M., Arencibia, A., Lindo, M. & Gascon, V. (2009), "Aqueous heavy metals removal by adsorption on amine-functionalized mesoporous silica", *J. Hazard. Mater.* 163, 213- 221.
- Anirudhan, T.S., Rijith, S. & Tharun, A. (2010), "Adsorptive removal of thorium(IV) from aqueous solutions using poly(methacrylic acid)-grafted chitosan/bentonite composite matrix: Process design and equilibrium studies", *Colloid Surface A*, 368, 13 -22.
- Bailliez, S., Nzihou, A., Beche, E. & Flamant, G. (2004), "Removal of Lead by Hydroxyapatite Sorbent, Process" *Saf. Environ. Protect.* 82, 175- 180.
- Bishnoi, N.R., Bajaj, M., Sharma, N. & Gupta, A. (2004), "Adsorption of Cr(VI) on activated rice husk carbon and activated alumina", *Bioresour. Technol.* 91, 305-307.
- Choi, S. & Jeong, Y. (2008), "The removal of heavy metals in aqueous solution by hydroxyapatite/cellulose composite", *Fiber Polym.* 9, 267-270.
- Corami, A., Mignardi, S. & Ferrini, V. (2007), "Copper and zinc decontamination from single and binary metal solutions using hydroxyapatite", *J. Hazard. Mater.* 146, 164-170.
- F.G. Simon, F.G., Birmann, V. & Peplinski, B. (2008), "Uranium removal from groundwater using hydroxyapatite", *Appl. Geochem.* 23, 2137-2145.
- Ghassabzadeh, H., Mostaeadi, M.T., Mohaddespour, A., Maragheh, M.G., Ahmadi, S.J. & Zaheri, P. (2010), "Characterizations of Co(II) and Pb(II) removal process from aqueous solutions using expanded perlite", *Desalination* 261, 73-79.
- Guibal, E., Milot, C., Etteradossi, O., Gauffier, C & Domard, A. (1999), "Study of molybdate ion sorption on chitosan gel beads by different spectrometric analyses", *Int. J. Biol. Macromol.* 24, 49-59.

- Günister, E., Pestreli, D., Ünlü, C.H., Atıcı, O. & Güngör, N. (2007), "Synthesis and characterization of chitosan-MMT bio-composite systems", *Carbohydr. Polym.* 67, 358-365.
- Hameed, B.H., Mahmoud, D.K. & Ahmad, A.L. (2008), "Equilibrium modeling and kinetic studies on the adsorption of basic dye by a low-cost adsorbent: Coconut (*Cocos nucifera*) bunch waste", *J. Hazard. Mater.* 158, 65-72.
- Han, Y., Lee, S., Choi, K., & Park, I. (2010), "Preparation and characterization of chitosan-clay nanocomposites with antimicrobial activity", *J. Phys. Chem. Solids* 71, 464-467 .
- Inglezakis, V.J., Stylianou, M.A., Gkantou, D. & Loizidou, M.D. (2007), "Removal of Pb(II) from aqueous solutions by using clinoptilolite and bentonite as adsorbents", *Desalination*, 210, 248-265.
- Katima, I. & Rodriguez, E. (2001), "Absorption of metal ions and swelling properties of poly(acrylic acid-co-itaonic acid) hydrogels", *J. Macromol. Sci. A*, 38, 543-558.
- Mobasherpour, I., Salahi, E. & Pazouki, M. (2011), "Removal of nickel (II) from aqueous solutions by using nano-crystalline calcium hydroxyapatite", *J. Saudi. Chem. Soc.* 15, 105-112.
- Motsi, T., Rowson, N.A. & Simmons, M.H. (2009), "Adsorption of heavy metals from acid mine drainage by natural zeolite", *Int. J. Miner. Process.* 92, 42-48.
- Pandey, S. & Mishra, S.B., Organic-inorganic hybrid of chitosan/organoclay nanocomposites for hexavalent chromium uptake, *J. Colloid. Interf. Sci.* 361(2011) 509-520.
- Paulino, A.T., Guilherme, M.R., Reis, A.V., Tambourgi, E.B., Nozaki, J. & Muniz, E.C. (2007), "Capacity of adsorption of Pb<sup>2+</sup> and Ni<sup>2+</sup> from aqueous solutions by chitosan produced from silkworm chrysalides in different degrees of deacetylation", *J. Hazard. Mater.* 147, 139-147.
- Pawlak, A. & Mucha, M. (2003), "Thermogravimetric and FTIR studies of chitosan blends", *Thermochim. Acta*, 396, 153- 166.
- Ray, S.S. & Okamoto, M. (2003), "Polymer/layered silicate nanocomposites: a review from preparation to processing", *Prog. Polym. Sci.* 281539-1641.
- Raynaud, S., Champion, E., Assollant, D.B. & Thomas, P. (2002), "Calcium phosphate apatites with variable Ca/P atomic ratio I. Synthesis, characterisation and thermal stability of powders", *Biomaterials* 23, 1065-1072.
- Seo, J.W. & B. K. Kim, B.K. (2005), "Preparations and Properties of Waterborne Polyurethane / Nanosilica Composites", *Polym. Bull.* 54, 123-128.
- Smicklas, I., Dimovic, S., Plecas, P. & Mitric, M. (2006), Removal of Co<sup>2+</sup> from aqueous solutions by hydroxyapatite", *Water Res.* 40, 2267-2274.
- Song, L., Hu, Y., Tang, Y., Zhang, R., Chen, Z. & Fan, W. (2005), "Study on the properties of flame retardant polyurethane /organoclay nanocomposite", *Polym. Degrad. Stab.* 87, 111-116.
- Sun, T.M. & Garces, J.M. (2002), "High-Performance Polypropylene-Clay Nanocomposites by In-situ Polymerization with Metallocene/Clay Catalysts", *Adv. Mater.* 14, 128-130.
- Sundaram, C.S., Viswanathan, N. & Meenakshi, S. (2008), "Calcium phosphate apatites with variable Ca/P atomic ratio I. Synthesis, characterisation and thermal stability of powders", *Bioresour. Technol.*, 99, 8226- 8230.
- Tianwei, T., Xiaojing, H., & Weixia, D. (2001), "Adsorption behaviour of metal ions on imprinted chitosan resin", *J. Chem Technol Biotechnol* , 76, 191-195.
- Vaia, R.A. (2000), "In Polymer-Clay Nanocomposites" ; Pinnavaia, T. J.; Beall, G.W. (Eds.), Wiley: New York, 244-263.
- Xu, H.Y., Yang, L., Wang, P., Liu, Y. & Peng, M.S. (2008), "Kinetic research on the sorption of aqueous lead by synthetic carbonate hydroxyapatite", *J. Environ. Manage.* 86319-328.
- Yao, K.J., Song, M., Hourston, D.J. & Luo, D.Z. (2002), "Polymer/layered clay nanocomposites: 2 polyurethane nano-composites", *Polymer* 43, 1017-1020 .
- Zaini, M.A. & Amano, M. Machida (2010), "Adsorption of heavy metals onto activated carbons derived from poly-

acrylonitrile fiber”, J. Hazard. Mater., 180, 552-560.

Zheng, Y. & Wang, A. (2009), “Evaluation of ammonium removal using a chitosan-g-poly (acrylic acid)/rectorite hydrogel composite”, J. Hazard. Mater., 171, 671-677.

Zhu, R., Yu, R., Yao, J., Mao, D., Xing, C. & Wang, D. (2008), “Removal of Cd<sup>2+</sup> from aqueous solutions by hydroxy-apatite”, Catal. Today, 139, 94-99.

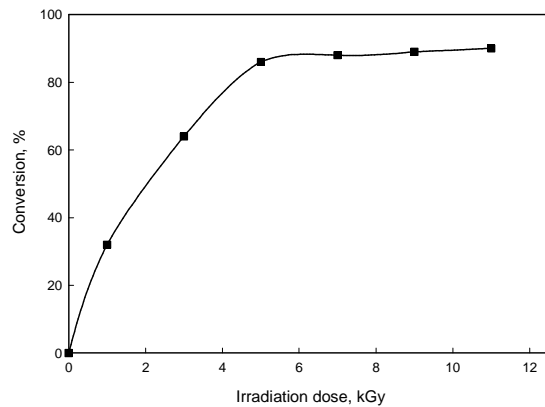


Fig.1. Effect of irradiation dose on the monomer conversion percent of MACB composite.

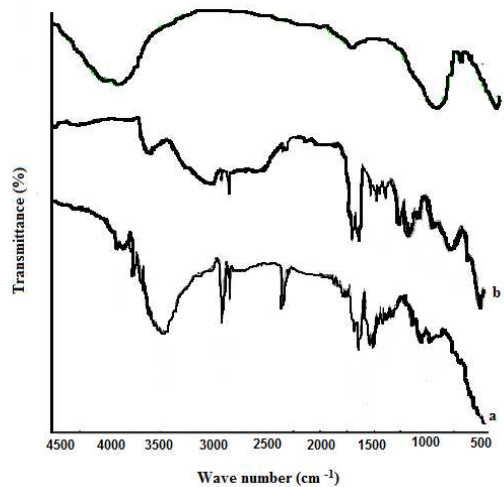


Fig.2. FTIR spectra of chitosan (a) MACB composite (b) and bentonite (c).

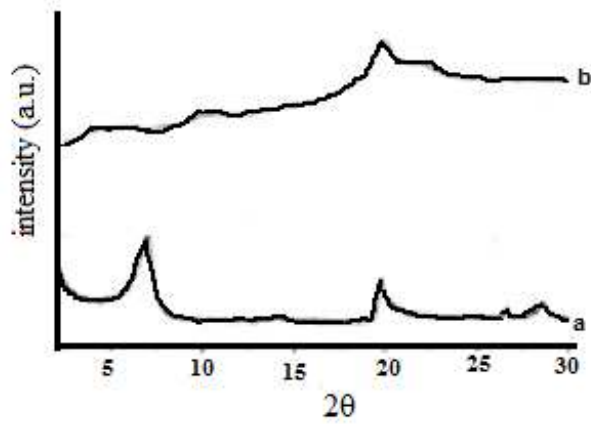


Fig.3. XRD spectra of bentonite (a) and MACB composite (b).

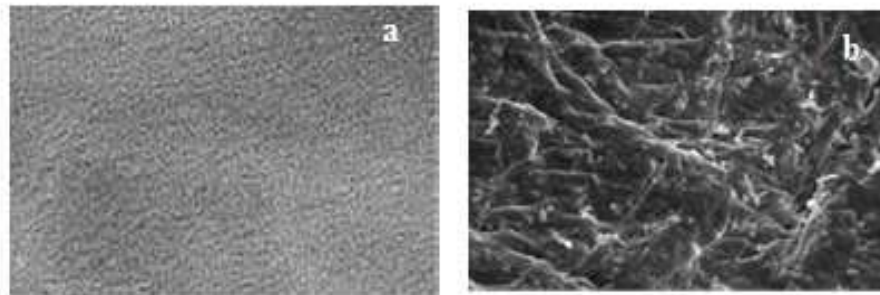


Fig.4. SEM micrograph of bentonite (a) and MACB composite (b)

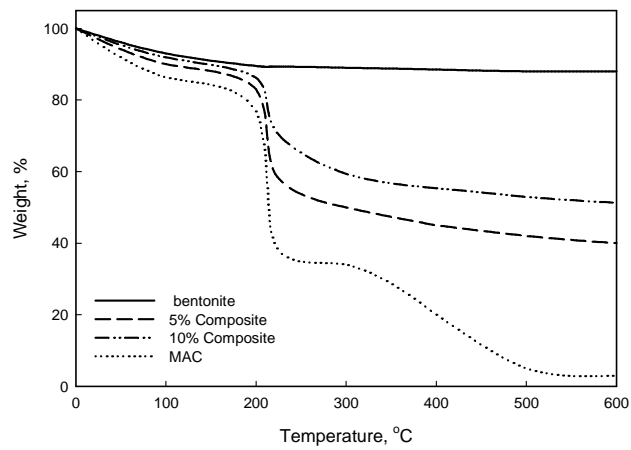


Fig.5. TGA of bentonite, MAC and MACB composites with different bentonite content.

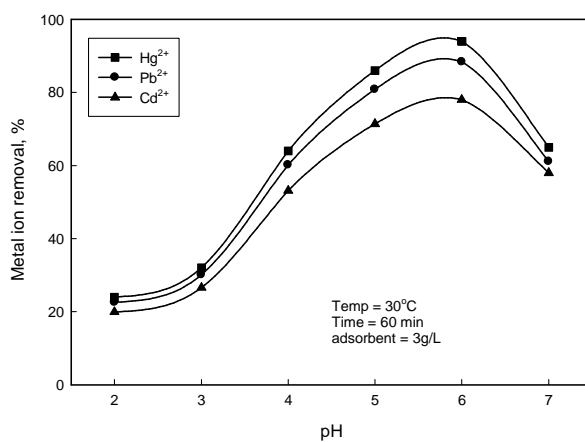


Fig.6. Effect of pH on removal of Hg<sup>2+</sup>, Pb<sup>2+</sup> and Cd<sup>2+</sup> onto MACB composite.

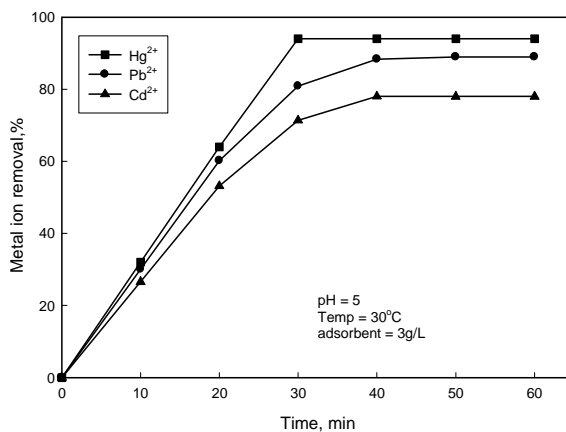


Fig.7. Effect of contact time on removal of Hg<sup>2+</sup>, Pb<sup>2+</sup> and Cd<sup>2+</sup> onto MACB composite.

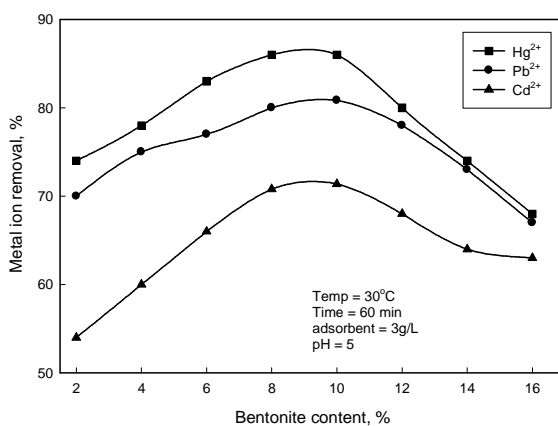


Fig.8. Effect of bentonite content on removal of Hg<sup>2+</sup>, Pb<sup>2+</sup> and Cd<sup>2+</sup> onto MACB composite.

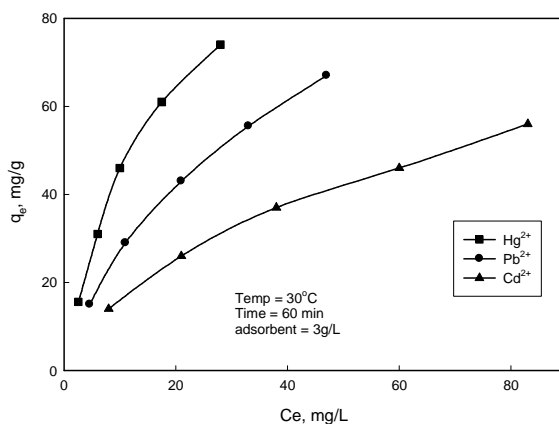


Fig.9. Effect of equilibrium concentration on adsorption of Hg<sup>2+</sup>, Pb<sup>2+</sup> and Cd<sup>2+</sup> onto MACB composite.

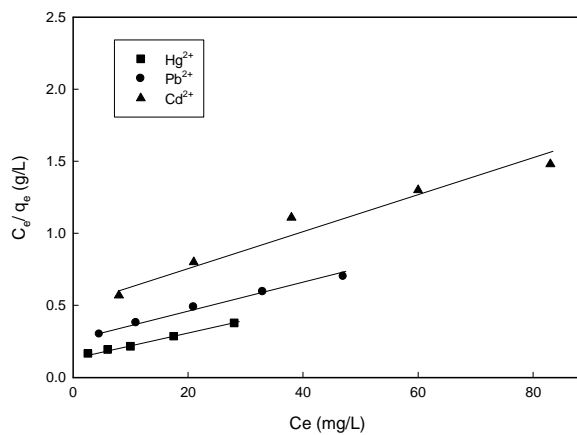


Fig.10. Langmuir isotherm for adsorption of Hg<sup>2+</sup>, Pb<sup>2+</sup> and Cd<sup>2+</sup> onto MACB composite.

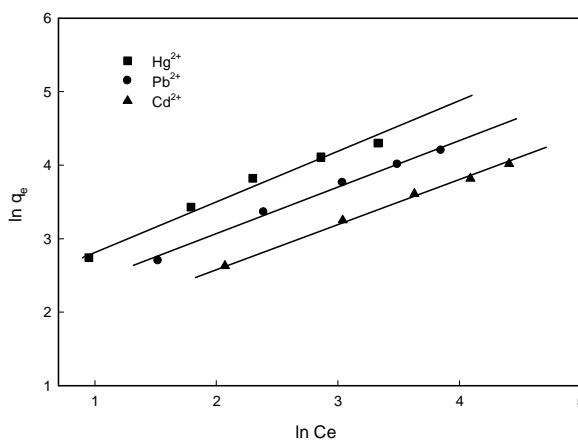


Fig.11. Freundlich isotherm for adsorption of Hg<sup>2+</sup>, Pb<sup>2+</sup> and Cd<sup>2+</sup> onto MACB composite.

**Table 1:** Langmuir and Freundlich constants for  $\text{Hg}^{2+}$ ,  $\text{Pb}^{2+}$  and  $\text{Cd}^{2+}$  adsorption onto MACB composite.

Metal ions	Langmuir constants			Freundlich constants		
	$q_{\max}$ (mg/g)	b (L/mg)	$R^2$	$K_F$ [mg/g (mg/L) <sup>-1/n</sup> ]	n	$R^2$
$\text{Hg}^{2+}$	125	0.17	0.9972	8.98	1.51	0.9802
$\text{Pb}^{2+}$	111	0.30	0.9911	5.87	1.56	0.9941
$\text{Cd}^{2+}$	83	0.46	0.9599	4.19	1.70	0.9973

This academic article was published by The International Institute for Science, Technology and Education (IISTE). The IISTE is a pioneer in the Open Access Publishing service based in the U.S. and Europe. The aim of the institute is Accelerating Global Knowledge Sharing.

More information about the publisher can be found in the IISTE's homepage:

<http://www.iiste.org>

## CALL FOR PAPERS

The IISTE is currently hosting more than 30 peer-reviewed academic journals and collaborating with academic institutions around the world. There's no deadline for submission. **Prospective authors of IISTE journals can find the submission instruction on the following page:** <http://www.iiste.org/Journals/>

The IISTE editorial team promises to review and publish all the qualified submissions in a **fast** manner. All the journals articles are available online to the readers all over the world without financial, legal, or technical barriers other than those inseparable from gaining access to the internet itself. Printed version of the journals is also available upon request from readers and authors.

### IISTE Knowledge Sharing Partners

EBSCO, Index Copernicus, Ulrich's Periodicals Directory, JournalTOCS, PKP Open Archives Harvester, Bielefeld Academic Search Engine, Elektronische Zeitschriftenbibliothek EZB, Open J-Gate, OCLC WorldCat, Universe Digital Library, NewJour, Google Scholar

